# Superconductivity and magnetism in heavy-fermion $UPd_2(Al,Ga)_3$

S. Süllow, B. Ludoph, B. Becker, G. J. Nieuwenhuys, A. A. Menovsky, and J. A. Mydosh
*Kamerlingh Onnes Laboratory, Leiden University, 2300 RA Leiden, The Netherlands*
(Received 8 October 1996)

We present bulk properties (resistivity, specific heat, and susceptibility) of the quasiternary system $UPd_2(Al_{1-x}Ga_x)_3$ and derive the superconducting and magnetic phase diagrams. For low Ga substitution ($x \leqslant 0.25$) a complete suppression of superconductivity is found, while the magnetic properties are hardly affected. For larger $x$ the magnetic transition temperature $T_N$ gradually decreases, and the mass enhancement of the electrons increases, until at $x=0.8$–$0.9$ a crystallographic transition takes place from the $PrNi_2Al_3$ to the $BaB_2Pt_3$ lattice. At the structural transition $T_N$ discontinuously increases, while the electronic specific heat $\gamma$ grows smoothly through the transition. We discuss the relationship between the alloying parameter $x$ and the magnetic ordering and electronic hybridization, respectively. The strong suppression of the superconductivity in $UPd_2Al_3$ with Ga suggests an unconventional mechanism of superconductivity, most probably related to spin fluctuations mediating the pairing. [S0163-1829(97)01126-0]

## I. INTRODUCTION

Hexagonal 123 compounds $UT_2M_3$, $T$=Ni and Pd and $M$=Al or Ga, were the subject of many detailed investigations in recent years for two main reasons:[1–3] The first is the appearance of heavy-fermion superconductivity in $UNi_2Al_3$ (Ref. 1) and $UPd_2Al_3$ (Ref. 2) (both crystallizing in the $PrNi_2Al_3$ lattice), and the second relates to the competition between the Kondo effect and magnetic interaction.

Heavy-fermion superconductivity is a topic of major interest in current research, since the superconductivity is carried by strongly correlated electrons which also mediate and transmit the magnetic interactions (for a review see Ref. 4). Here the pairing mechanism of the superconductivity might be different from that of the conventional phonon-coupled BCS superconductors; for instance, magnetic correlations or spin fluctuations could be involved.

Recently, we presented the basic properties of $UPd_2Ga_3$,[3] an allomorph to $UPd_2Al_3$. This system crystallizes in the $BaB_2Pt_3$ structure, which is a superstructure of the $PrNi_2Al_3$ lattice. Its general properties qualitatively resemble those of $UPd_2Al_3$. Quantitatively, the electronic specific heat $\gamma$ is larger, while the magnetically ordered moment $\mu_{\mathrm{ord}}$, transition temperature $T_N$, and the crystalline electric field (CEF) splitting of the low-lying levels are all smaller. Nevertheless, $UPd_2Ga_3$ was not found to be superconducting down to 50 mK. Hence, the replacement of Al in $UPd_2Al_3$ by Ga mainly affects the superconducting behavior, while the magnetism is hardly influenced. In order to investigate the dependence of $UPd_2(Al,Ga)_3$ on the local site symmetry of the uranium, alloying experiments using $UPd_2(Al_{1-x}Ga_x)_3$ have been performed. Here we can track the major differences between $UPd_2Ga_3$ and $UPd_2Al_3$ arising from (a) chemical pressure and (b) the superstructure, and their effect on the characteristic electronic parameters ($T_N$, $T_c$, $\gamma$, CEF, $\mu_{\mathrm{ord}}$).

In addition, the alloying experiments yield important information regarding the competition between magnetic exchange and the Kondo effect. The question is in how far a simple concept like the Doniach model[5] can be employed to describe the behavior of U compounds. Previously, it has been shown that the Doniach model qualitatively accounts for the magnetic properties of the 122 compounds.[6] The circumstances allowing the use of the Doniach model seem to arise from the crystallographic and magnetic structure. The 122 compounds crystallize in tetragonal structures and the kind of magnetic ordering appearing in these systems is of the Ising type (AF-I structure). Effectively, this situation creates a strong uniaxial anisotropy, which mimics the one dimensionality of the Doniach model.

In the 123 metals the crystallographic and magnetic anisotropies cannot simply be projected onto a quasi-one-dimensional picture, and a similar description of the physics based solely on the Doniach model does not properly account for the observed properties. Accordingly, Mentink *et al.*[7] proposed a model that still relies on the basic Doniach picture, but is more elaborate by introducing two different interactions governing the RKKY exchange and the Kondo effect.

In this paper we report our bulk measurements on the alloying series $UPd_2(Al_{1-x}Ga_x)_3$. In Sec. II we present the metallurgical analysis of the compounds, and in Sec. III the normal-state resistivity, specific heat, and susceptibility will be described. The evolution of magnetism with alloying is interpreted in terms of the competition between magnetism and the Kondo effect, incorporating the effect of Ga alloying on the CEF splitting. In Sec. IV the superconducting properties of $UPd_2(Al_{1-x}Ga_x)_3$ will be addressed. As a major result we find a complete suppression of superconductivity for small amounts of Ga alloying, contrasting the ineffectiveness of such Ga alloying on the magnetic properties. This observation we take as indication that $UPd_2Al_3$ is an unconventional superconductor, with a pairing mechanism based presumably on spin fluctuations.

## II. METALLURGY

All samples are polycrystals, formed by arc-melting the constituents (purity at least 99.9%) in stoichiometric ratio on

 

TABLE I. Sample composition (normalized to U=1), amount of second phases, lattice parameters and volume of the unit cells of $UPd_2(Al_{1-x}Ga_x)_3$.

| Composition | $x$ | % second | $a$ [Å] | $c$ [Å] |
|---|---|---|---|---|
| $UPd_{1.84}Al_{2.84}$ | 0 | 5 | 5.368(2) | 4.188(2) |
| $UPd_{1.87}Al_{2.70}Ga_{0.05}$ | 0.01 | 1 | 5.362(2) | 4.186(2) |
| $UPd_{1.85}Al_{2.60}Ga_{0.12}$ | 0.02 | 1 | 5.362(5) | 4.184(5) |
| $UPd_{1.87}Al_{2.73}Ga_{0.20}$ | 0.05 | 1 | 5.356(4) | 4.185(5) |
| $UPd_{1.98}Al_{2.57}Ga_{0.29}$ | 0.1 | 5 | 5.353(4) | 4.188(3) |
| $UPd_{1.97}Al_{2.46}Ga_{0.41}$ | 0.15 | 3 | 5.347(5) | 4.187(4) |
| $UPd_{1.97}Al_{2.27}Ga_{0.55}$ | 0.2 | 5 | 5.344(4) | 4.187(4) |
| $UPd_{2.02}Al_{1.93}Ga_{0.93}$ | 0.33 | 5 | 5.336(5) | 4.196(5) |
| $UPd_{2.00}Al_{0.92}Ga_{1.91}$ | 0.66 | 5 | 5.322(6) | 4.212(6) |
| $UPd_{2.03}Al_{0.44}Ga_{2.41}$ | 0.8 | 11 | 5.323(4) | 4.227(5) |
| $UPd_{2.02}Al_{0.23}Ga_{2.63}$ | 0.9 | 13 | 5.303(3) | 8.469(8) |
| $UPd_2Ga_{2.88}$ | 1 | 5 | 5.3015(1) | 8.5112(3) |

a water-cooled copper crucible. Subsequently, they have been annealed in high vacuum in quartz ampoules at 900 °C for 1 week. The weight losses of the samples have been monitored after melting and annealing, and were found to be negligible. All materials were checked by electron probe microanalysis (EPMA) and x-ray diffraction for composition and crystallographic structure.

The analysis of $UPd_2(Al_{1-x}Ga_x)_3$, $0 \leqslant x \leqslant 1$, indicated good homogeneity (as evinced by the small percentage of second phase; see Table I) for $x \leqslant 0.66$ and slightly less homogeneity for $x = 0.8$ and 0.9. (The latter samples were considered to be sufficiently pure for the purposes of our comparative study.) The compositions of the matrices, measured by EPMA, are also listed in Table I. The total of Ga plus Al concentration adds up to about 2.8–2.9 instead of 3, probably indicating preferential Ga/Al evaporation during melting.

The lattice parameters and unit-cell volumes of the compounds are included in Table I. The $PrNi_2Al_3$ structure was found for compositions $x \leqslant 0.8$. However, $UPd_2Al_{0.3}Ga_{2.7}$ ($x = 0.9$) forms in the $BaB_2Pt_3$ superstructure, implying that the crystallographic transition from the $PrNi_2Al_3$ to the $BaB_2Pt_3$ lattice occurs between $x = 0.8$ and 0.9. In Fig. 1

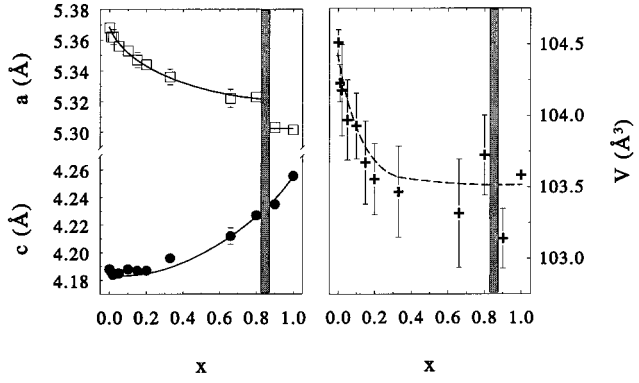


FIG. 1. The lattice parameters $a$ (□) and $c$ (●), and the volume of the unit cell $V$ (+) of $UPd_2(Al_{1-x}Ga_x)_3$ vs Ga concentration $x$. The shaded bars between $x = 0.8$ and 0.9 mark the structural transition. The lines are guides to the eye.

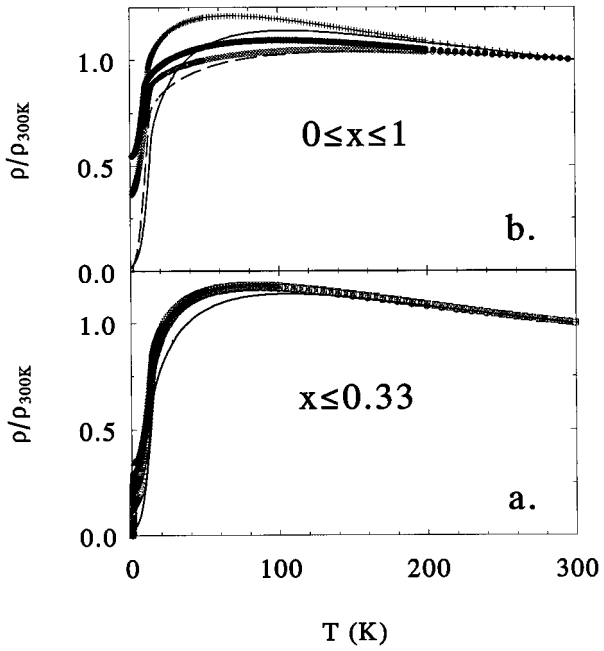


FIG. 2. (a) The normalized resistivity of $UPd_2(Al_{1-x}Ga_x)_3$ for $x = 0$ (–), 0.05 (○), 0.1 (▽), 0.2 (□), and 0.33 (△). (b) As for (a), but now for $x = 0$ (–), 0.66 (+), 0.8 (●), 0.9 (◇), and 1 (– –).

the $a$ and $c$ axis parameters are plotted against Ga concentration $x$ (for $x = 0.9$ and 1, one-half the $c$ axis values are given). Initially, for low Ga concentrations, the $a$ axis decreases linearly, but pronounced deviations from linearity are found at the transition from the $PrNi_2Al_3$ to the $BaB_2Pt_3$ structure. In contrast, the $c$ axis shows hardly any increase for $x \leqslant 0.2$, while it rises rapidly for larger $x$ without a distinct anomaly at the structural transition. The overall effect of the complete Ga substitution on the unit-cell volume is equivalent to an applied pressure of about 10 kbar.[3]

### III. MAGNETISM IN $UPd_2(Al_{1-x}Ga_x)_3$

In Fig. 2 the overall normalized resistivities for $UPd_2(Al_{1-x}Ga_x)_3$ are displayed. All samples $UPd_2(Al_{1-x}Ga_x)_3$ were quite brittle, and we could not determine absolute resistivity values with high accuracy. However, for $x \leqslant 0.33$ there is little difference in the normalized resistivities between 100 and 300 K, implying that $\rho_{300\,K}$ is similar for all samples in this alloying range (about 180 $\pm 10\ \mu\Omega$ cm). For higher Ga concentrations this overlap does not occur and we can only estimate $\rho_{300\,K}$ to about 200 $\pm 50\ \mu\Omega$ cm.

Since for $x \leqslant 0.33$ the normalized resistivities are virtually indistinguishable above 100 K [Fig. 2(a)], the physical mechanism governing the resistivity is not altered for low amounts of Ga substitution. Only below 100 K do the curves for different $x$ begin to deviate from each other mainly due to the collapse of lattice periodicity. The degree of lattice disorder is, to first approximation, measured by the residual resistivity ratio $RRR = \rho_{300\,K}/\rho_{2\,K}$, which is strongly suppressed with increasing $x$. The magnetic transition temperature, in contrast, is barely affected by Ga alloying. In Fig.

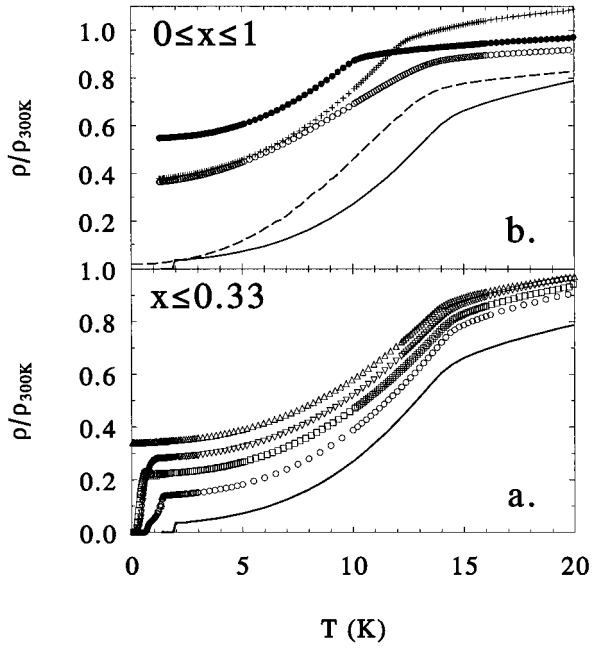


FIG. 3. (a) The antiferromagnetic transition in the normalized resistivity of $UPd_2(Al_{1-x}Ga_x)_3$ for $x = 0$ (–), 0.05 (○), 0.1 (▽), 0.2 (□), and 0.33 (△). (b) As for (a), but now for $x = 0$ (–), 0.66 (+), 0.8 (●), 0.9 (◇), and 1 (– –).

3(a) the low-$T$ region of the normalized resistivity is enlarged for all samples with $x \leqslant 0.33$. The transition temperatures $T_N$ (determined as minimum in $d^2\rho/dT^2$) are about 14.1 – 14.5 K (see Table II).

A different situation is encountered as the Ga concentration is increased above $x \approx 0.33$, as shown in Figs. 2(b) and 3(b) (the values of $T_N$ and RRR are included in Table II). Here the general shape of the curves and $T_N$ shows a pronounced dependence on $x$. The changing shapes of the curves imply that the CEF splitting shifts with alloying from that of $UPd_2Al_3$ to $UPd_2Ga_3$. Further, using the RRR as a measure for disorder, it is reasonable that pure $UPd_2Ga_3$ exhibits a much larger RRR than the alloyed samples. The most remarkable result, however, is an anomaly in the $T_N$ vs $x$ dependence. We find a jumplike increase of $T_N$ at the structural transition between $x = 0.8$ and 0.9. This implies that the crystallographic superstructure directly affects the magnetic exchange in $UPd_2Ga_3$.

TABLE II. Antiferromagnetic transition temperatures $T_N$ (derived from normalized resistivity $\rho/\rho_{300\,K}$, specific heat $c_p$, and susceptibility $\chi_{dc}$), superconducting transition temperatures $T_c$, the residual resistivity ratio RRR = $\rho_{300\,K}/\rho_{2\,K}$, and the electronic specific heat coefficient $\gamma$ for $UPd_2(Al_{1-x}Ga_x)_3$.

| $x$ | $T_{N;\rho}$ (K) | $T_{N;c_p}$ (K) | $T_{N;\chi}$ (K) | $T_c$ (K) | RRR | $\gamma$ (J/mole K$^2$) |
|---|---|---|---|---|---|---|
| 0 | 14.3 | 14.3 | 13.8 | 1.89 | 28 | 0.148(5) |
| 0.01 | 14.5 | — | — | 1.64 | 18 | – |
| 0.02 | 14.5 | — | 13.9 | 1.51 | 9.4 | – |
| 0.05 | 14.5 | — | 13.9 | 1.15 | 7.0 | – |
| 0.1 | 14.5 | 14.3 | 13.7 | 0.52 | 3.5 | 0.149(5) |
| 0.15 | 14.5 | — | 13.5 | 0.76 | 4.0 | – |
| 0.2 | 14.4 | 14.0 | 13.6 | 0.33 | 4.4 | 0.144(5) |
| 0.33 | 14.1 | 13.2 | 13.2 | $< 0.05$ | 2.9 | 0.147(5) |
| 0.66 | 12.3 | 11.6 | 11.5 | $< 0.05$ | 2.6 | 0.184(5) |
| 0.8 | 10.2 | 9.7 | 9.46 | $< 0.05$ | 1.8 | 0.191(5) |
| 0.9 | 13.5 | 12.8 | 12.0 | $< 0.05$ | 2.7 | 0.226(5) |
| 1 | 13.1 | 13 | 12.2 | $< 0.05$ | 30 | 0.230(5) |

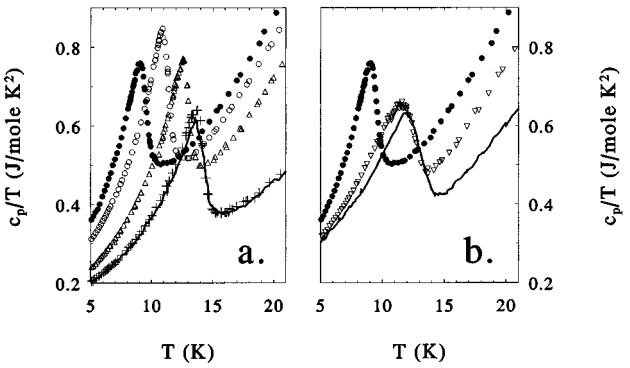


FIG. 4. (a) The specific heat divided by temperature $c_p/T$ vs temperature $T$ of $UPd_2(Al_{1-x}Ga_x)_3$ with $x = 0$ (–), 0.1 (+), 0.33 (△), 0.66 (○), and 0.8 (●), and (b) with $x = 0.8$ (●), 0.9 (▽), and 1 (–).

In addition, we studied the antiferromagnetic transitions of $UPd_2(Al_{1-x}Ga_x)_3$ by specific heat (depicted as $c_p/T$ against $T$ in Fig. 4). The peaks of the transition are clearly visible; the transition temperatures $T_N$, determined by entropy balance, are included in Table II. Although these are slightly lower than those obtained from the resistivity, the major feature, the jump of $T_N$ at the structural transition, reproduces well.

For $x \leqslant 0.2$ little effect of the Ga substitution is resolvable in the specific heat, if compared to $UPd_2Al_3$ [Fig. 4(a)]. Further, the shape of the antiferromagnetic transition is not strongly altered with the replacement of Al by Ga for $x \leqslant 0.8$, but it suddenly broadens after the structural transition [Fig. 4(b)]. Also, the absolute values of $c_p$ above $T_N$ go through a maximum at the structural transition. Both effects can partially be attributed to a shift of the energy splitting of the low-lying CEF levels with Ga alloying. We have already described the dependence of the shape of the magnetic transition in $c_p$ on the particular CEF level scheme in Ref. 8. Further, the maximum of the absolute $c_p$ values above $T_N$ for $x = 0.8$ indicates that the CEF energy splitting does not change linearly with Ga substitution, but that there is an anomaly of the level splitting at the transition from the $PrNi_2Al_3$ to the $BaB_2Pt_3$ lattice (with the introduction of the superstructure the electric field gradients at the U site, and thus the CEF scheme, will be affected). In addition to this CEF shift with $x$, there is also an effect of the Ga alloying on the phonon spectrum. At present, we cannot assess from the specific heat the full extent of the changes in the CEF scheme or the phonon spectrum and are unable to quantify these modifications.

For all samples $c_p/T$ is linear in $T^2$ below the magnetic transition regime at $T_N$, and therefore, we can derive the electronic specific heat $\gamma$ as function of $x$. The values of $\gamma$ for $UPd_2(Al_{1-x}Ga_x)_3$ (extrapolated between 2 and 10 K for $x = 0$ and 1, 4.5, and 10 K for $0 < x < 0.8$ and $x = 0.9$, and

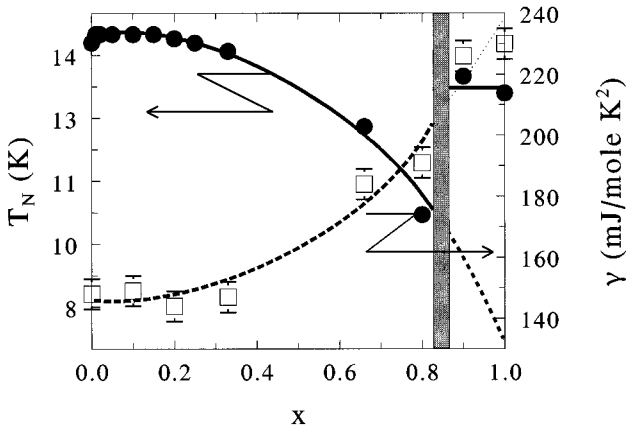


FIG. 5. The antiferromagnetic phase diagram (●) for $UPd_2(Al_{1-x}Ga_x)_3$ (from the resistivity) and the electronic contribution to the specific heat $\gamma$ (□).

4.5 and 8 K for $x = 0.8$) are included in Table II and plotted in Fig. 5. The plot illustrates the evolution of $T_N$ (derived from $\rho/\rho_{300\,K}$) and $\gamma$ with $x$ for $UPd_2(Al_{1-x}Ga_x)_3$. The shaded region in the diagram denotes the structural transition regime. From the figure it is obvious that $\gamma$ does not scale with $T_N$ over the whole alloying range. We will reconsider this feature in the discussion.

Finally, we measured the susceptibility of $UPd_2(Al_{1-x}Ga_x)_3$ (Fig. 6). The antiferromagnetic transition temperatures (determined from the maximum in $d(\chi T)/dT$) are included in Table II and exhibit, as the specific heat and the resistivity, an anomaly of $T_N$ between $x = 0.8$ and 0.9. Also, we find a close connection between the shape of $\chi$ and the Ga alloying. For $x \leqslant 0.2$ little change in the shape of $\chi$ is seen (not shown). Then, for $0.33 \leqslant x \leqslant 0.8$, the height of the maximum in $\chi$ increases, the maximum shifts to lower temperatures, and its shape is preserved. Suddenly, at the structural transition, the shape is altered as well, and the CEF maximum coincides with the antiferromagnetic transition.

The dependence of $\chi$ can be understood in terms of the CEF splitting. In order to illustrate this, we apply the CEF model, used to simulate $c_p$ of $UPd_2Ga_3$ in Ref. 8, and calculate the susceptibility. The results are shown in Fig. 7, and they give a general impression of the dependence of $\chi$ on the CEF splitting for $UPd_2Ga_3$, $UPd_2Al_3$, and the intermediate case of $UPd_2(Al_{0.2}Ga_{0.8})_3$. The CEF splitting consists of a singlet ground state $\Delta_0$ and an excited singlet $\Delta_1$, mixing with a doublet $\Delta_2$ at higher temperatures.[9] The energy splittings are given in the plot.

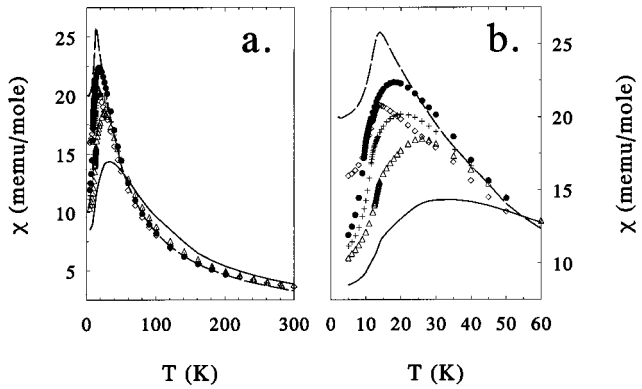


FIG. 6. The susceptibility $\chi$ below 300 K (a) and 60 K (b) of $UPd_2(Al_{1-x}Ga_x)_3$ with $x = 0$ (–), 0.33 (△), 0.66 (+), 0.8 (●), 0.9 (◇), and 1 (– –).

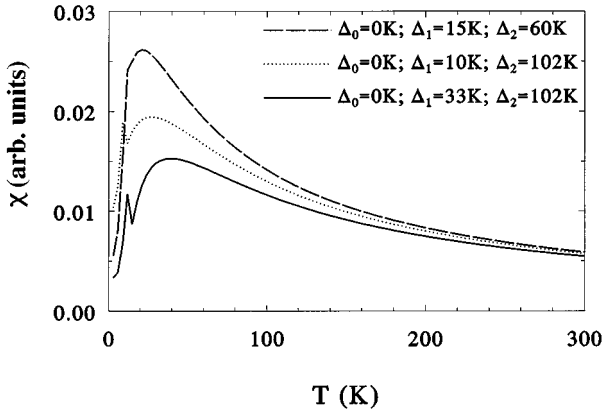


FIG. 7. A molecular field simulation of the susceptibility of $UPd_2(Al_{1-x}Ga_x)_3$ according to the CEF scheme described in the text, with the splitting energies given in the plot. The three calculations correspond to the cases of $UPd_2Al_3$ (–), $UPd_2Ga_3$ (– –), and $UPd_2(Al_{0.2}Ga_{0.8})_3$ (· · ·).

As with all simple mean-field models, there are deficiencies. No short-range order fluctuations at $T_N$ have been introduced, and we find the calculated antiferromagnetic peaks not fully matching the experimental observations. Moreover, the heavy-fermion Pauli paramagnetism and the high-lying CEF levels are disregarded. Still, the model reproduces the main features of the experiment. From the calculation the general trend of alloying from $UPd_2Al_3$ to $UPd_2Ga_3$ is to shift the CEF maximum below the magnetic transition of $UPd_2Ga_3$. The ratio of maxima for different $x$ is properly described. Finally, the anomalous CEF behavior at the structural transition seems to indicate that with Ga alloying for $x \leqslant 0.8$ (in the $PrNi_2Al_3$ structure) the splitting between the ground state $\Delta_0$ and the excited singlet $\Delta_1$ diminishes. After the structural transition the splitting between $\Delta_0$ and the doublet $\Delta_2$ decreases, while $\Delta_1$ increases slightly.

We now return to the phase diagram shown in Fig. 5. Obviously, $T_N$ and $\gamma$ scale as long as the $PrNi_2Al_3$ structure is preserved. The decrease of $T_N$, signifying a weakening of magnetism and a reduction of the ordered magnetic moment, is accompanied by the increase of $\gamma$. However, at the structural transition $T_N$ exhibits a jumplike increase, indicating that the magnetic exchange is strengthened. In contrast, we do not find a similar anomaly in $\gamma$, which instead increases (possibly with a small upward jump) through the structural transition. Apparently, the hybridization is not strongly dependent on the U local site symmetry.

This finding implies that a description of the alloy system $UPd_2(Al_{1-x}Ga_x)_3$ entirely in terms of the Doniach model fails. The structural changes in the system, which heavily affect the magnetism, cannot be accounted for in this model. Only as long as the $PrNi_2Al_3$ structure is kept can the scaling between $\gamma$ and $T_N$ be qualitatively described within a Doniach-like picture. In our opinion the evolution of magne-

tism in $UPd_2(Al_{1-x}Ga_x)_3$ can be elucidated in a phenomenological model as follows.

(a) The hybridization exchange $J_{f\text{-}s,p,d}$ depends mainly on the unit-cell volume. It is not (or only weakly) dependent on the details of the crystallographic structure, but primarily related to the distance between the magnetic and metallic atoms. Its value is determined by the volume of the unit cell and the average overlap of the U-metal orbitals. In the Doniach picture a hybridization energy scale is set by $J_{f\text{-}s,p,d}$ according to[5]

$$E_{f\text{-}s,p,d} \sim \frac{\exp\{-1/[N(0)J_{f\text{-}s,p,d}]\}}{N(0)}. \tag{1}$$

(b) Because of the simplicity of the magnetic structure in $UPd_2(Al_{1-x}Ga_x)_3$, viz., the antiferromagnetic arrangement along the $c$ axis of spins ferromagnetically coupled in the hexagonal basal plane, we can omit from further consideration the magnetic exchange in the hexagonal plane. Here the coupling is always ferromagnetic, as it is stabilized either through strong internal fields or simply by the hexagonal symmetry. This avoids problems with frustration or complex magnetic structures in the basal plane which could occur if the interactions were antiferromagnetic.[10,11] The crucial magnetic exchange along the $c$ axis seems to be well described by a usual RKKY oscillatory type of interaction $J_{\mathrm{RKKY}}(c)$. Its energy scale is set in the Doniach representation by

$$E_{\mathrm{RKKY}} \sim N(0)J^2_{\mathrm{RKKY}}(c). \tag{2}$$

Our model closely resembles the one proposed by Mentink *et al.*,[7] only we have removed the assumption of an anisotropic hybridization $J_{f\text{-}s,p,d}$.

Accordingly we can describe the observed evolution of the magnetic properties in $UPd_2(Al_{1-x}Ga_x)_3$: When alloying $UPd_2Al_3$ with Ga, the volume of the unit cell and the U-Pd distance (as leading term of the hybridization strength) decrease, and, correspondingly, $J_{f\text{-}s,p,d}$ and $\gamma$ increase. $J_{\mathrm{RKKY}}(c)$ (as long as the $PrNi_2Al_3$ structure is retained) decreases with the increasing $c$ axis. Both effects work in concord and $T_N$ is reduced.

At the structural transition the RKKY exchange is strongly affected and $T_N$ increases discontinuously. In contrast, $\gamma$ hardly exhibits any anomaly, since the average U-metal distances as well as the volume of the unit cell change smoothly through the structural transition. (As mentioned above, there might be a small jumplike increase of $\gamma$ at the transition; nevertheless, it does not affect our argument, as both $\gamma$ and $T_N$ increase, indicating the breakdown of scaling.) Proof that mainly $J_{\mathrm{RKKY}}(c)$ changes discontinuously at the transition is the hypothetical value of $T_N$ for superstructure-free $UPd_2Ga_3$. As noted in Ref. 3, there is a discrepancy between the decrease of $\mu_{\mathrm{ord}}$ and $T_N$ with full replacement of Al by Ga in $UPd_2Al_3$. While $\mu_{\mathrm{ord}}$ is 1.7 times smaller in $UPd_2Ga_3$ than in $UPd_2Al_3$, $T_N$ is lowered only by a factor 1.1. However, as is illustrated by the extrapolation of $T_N$ to $x = 1$, indicated in Fig. 5, the hypothetical value of $T_N$ for $UPd_2Ga_3$, crystallizing in the $PrNi_2Al_3$ structure, would be about 7 K. This reduction of $T_N$ would be in much better agreement with the reduction of $\mu_{\mathrm{ord}}$ and the increase of $\gamma$.

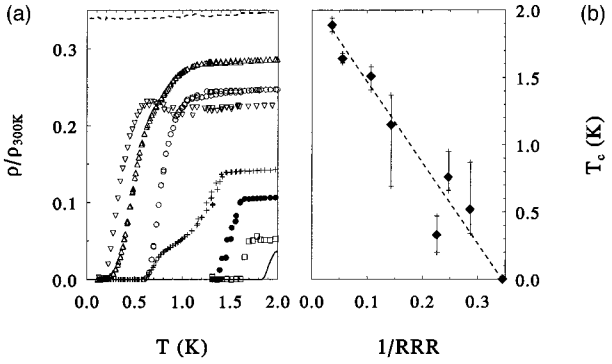


FIG. 8. (a) The superconducting transitions of $UPd_2(Al_{1-x}Ga_x)_3$: $x = 0$ (–), 0.01 (□), 0.02 (●), 0.05 (+), 0.1 (△), 0.15 (○), 0.2 (▽), and 0.33 (– –). (b) The relation between $T_c$ and the residual resistance ratio RRR. Bars indicate 10% and 90% points of the transitions.

## IV. SUPERCONDUCTIVITY IN $UPd_2(Al_{1-x}Ga_x)_3$

For small amounts of Ga the specimens of $UPd_2(Al_{1-x}Ga_x)_3$ still exhibit superconductivity. The superconducting transition temperatures are determined by resistivity measurements; the transition curves are depicted in Fig. 8(a). The transition temperatures (determined as the 50% point of the resistance drop) are included in Table II.

Several of the curves show broad and double transitions indicating metallurgical imperfections. In order to check if secondary phase superconductivity is the source of the transition broadening we compared the Meissner effect for several samples. These measurements indeed show that samples with $x > 0.1$ are not bulk superconductors, since they exhibit Meissner fractions only of about 10–20 %. For lower Ga concentrations, however, the samples are indeed bulk superconductors.

This finding implies that another experimental feature has to be taken with caution. From the resistance data it might be concluded that $T_c$ scales with the RRR. In Fig. 8(b) this is illustrated by plotting $T_c$ against RRR. In fact, such dependence has been claimed before, based on alloying experiments on $UPd_2Al_3$ with a large group of dopants.[12] Remarkably, the correlation between $T_c$ and RRR even holds reasonably well for $UPd_2(Al_{1-x}Ga_x)_3$ with $x > 0.1$, thus for nonbulk superconducting samples. Hence, for larger quantities of Ga substitution (and for other dopants?) the correlation between $T_c$ and RRR is fortuitous. Still, for low Ga amounts there exists a relation between the reduction of the RRR (being a measure of the mean free path in this Ga alloying range) and $T_c$. A similar relationship between mean free path and reduction of $T_c$ had been found for another heavy-fermion superconductor, $UPt_3$.[13]

We argue that the strong suppression of $T_c$ and the mean free path with Ga doping indicates unconventional superconductivity in $UPd_2Al_3$. This interpretation of the alloying experiments on $UPd_2(Al_{1-x}Ga_x)_3$ is based on the superconducting and magnetic phase diagrams (Fig. 9). While the magnetic behavior is unaffected by Ga alloying up to $x \approx 0.3$, superconductivity fully vanishes at $x = 0.25$. This indicates that the nonmagnetic Ga acts as an effective pair breaker (we ignore the problem of the broad superconducting transitions, since it does not affect the primary result of the

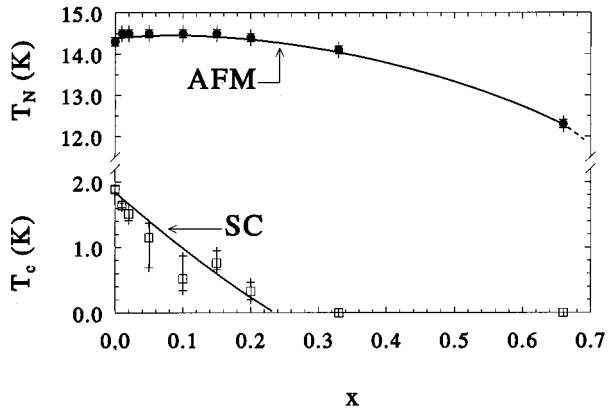


FIG. 9. Antiferromagnetic and superconducting phase diagrams of $UPd_2(Al_{1-x}Ga_x)_3$. $T_N$ and $T_c$ are both determined via resistance measurements.

*complete* suppression of superconductivity by Ga doping). Now, according to several authors, for unconventional superconductivity, the pair-breaking effect due to nonmagnetic impurities could be of the same order as that observed for magnetic ones in conventional superconductors.[14–16] In particular, Millis *et al.*[16] pointed out that a $T_c$ depression in unconventional superconductors by nonmagnetic pair breakers is coupled to the reduction of the mean free path of the electrons. Since up to an alloying rate of $x \leqslant 0.33$, apart from the RRR reduction, virtually no changes appear in the normal-state properties of $UPd_2(Al_{1-x}Ga_x)_3$—$T_N$, $\gamma$, and the CEF splitting remain essentially constant—we can safely assume that other pair-breaking mechanisms (for instance, magnetic ones) are not affected by the Ga alloying. Only the nonmagnetic pair breaking by the Ga can cause the dramatic suppression of $T_c$.

There is further evidence that this scenario applies to $UPd_2Al_3$. Millis *et al.*[16] investigated the pair-breaking effect of spin fluctuations in a *d*-wave superconductor and found that low-frequency spin fluctuations act as effective pair breakers, while the high-frequency spin fluctuations tend to be pair forming. A change in the spin fluctuation spectrum of a *d*-wave superconductor should therefore be reflected in $T_c$. From bulk data it is difficult to obtain accurate information on the spin fluctuation spectrum of a particular compound. Some insight can be gained from the low-temperature magnetic resistivity. For two similar magnetic compounds (like $UPd_2Al_3$ and $UPd_2Ga_3$) the $T^2$-coefficient of the resistivity $A$ reflects the spin fluctuations: The larger the value of $A$, the lower the average spin fluctuation frequency. Thus, in our case, the nonsuperconducting $UPd_2Ga_3$ should have a much larger value of $A$ than $UPd_2Al_3$, in agreement with experiment. While in $UPd_2Ga_3$ a value $A = 0.66$ $\mu\Omega$ cm/K$^2$ is reported,[3] for $UPd_2Al_3$ a significantly smaller value $A = 0.26$ $\mu\Omega$ cm/K$^2$ is found.[17]

Finally, recent NMR and NQR measurements on $UPd_2Ga_3$ and $UPd_2Al_3$ (Refs. 18–20) indicate pronounced differences in the spin fluctuation spectra of the two compounds. Unfortunately, from these measurements it could not be unambiguously concluded whether the average spin fluctuation frequency is higher in $UPd_2Al_3$ or $UPd_2Ga_3$. Further experiments and analysis are underway to clarify this point.

## V. CONCLUSIONS

Summarizing our results on $UPd_2(Al_{1-x}Ga_x)_3$ leads to the following conclusions.

(a) The magnetic properties of $UPd_2Al_3$, $UPd_2Ga_3$, and the intermediate quasiternary compounds are qualitatively similar. The small quantitative differences can be understood if the influence of the crystallographic superstructure on the RKKY exchange along the *c* axis is taken into account. As long as the $PrNi_2Al_3$ structure is preserved, the physical quantities $\gamma$, $T_N$, and $\mu_{\rm ord}$ scale with the Ga concentration. This scaling can be understood in a model utilizing the *c* axis RKKY exchange $J_{\rm RKKY}$ and the volume hybridization $J_{f\text{-}s,p,d}$. At the structural transition $J_{\rm RKKY}$ is strongly affected, while $J_{f\text{-}s,p,d}$ is not, leading to a breakdown of the scaling.

(b) The remarkable pair-breaking effect of nonmagnetic Ga is a strong indication for unconventional superconductivity. Here the absence of superconductivity in $UPd_2Ga_3$ would be attributed to differences in the spin fluctuation spectrum between $UPd_2Ga_3$ and $UPd_2Al_3$, which is qualitatively in agreement with experimental findings. Nevertheless, the final proof for unconventional superconductivity in $UPd_2Al_3$, namely, a quantitative comparison of the spin fluctuation spectra of $UPd_2Al_3$ and $UPd_2Ga_3$, is still lacking.

## ACKNOWLEDGMENTS

We gratefully acknowledge the experimental assistance of S. Ramakrishnan and C. C. Mattheus as well as fruitful discussions with S.A.M. Mentink. The samples have been made by FOM-ALMOS. Part of this research was performed under the auspices of the Nederlandse Stichting voor Fundamenteel Onderzoek der Materie (FOM).

[1] C. Geibel, S. Thies, D. Kaczorowski, A. Mehner, A. Grauel, B. Seidel, U. Ahlheim, R. Helfrich, K. Petersen, C. D. Bredl, and F. Steglich, Z. Phys. B **83**, 305 (1991).

[2] C. Geibel, C. Schank, S. Thies, H. Kitazawa, C. D. Bredl, A. Böhm, M. Rau, A. Grauel, R. Caspary, R. Helfrich, U. Ahlheim, G. Weber, and F. Steglich, Z. Phys. B **84**, 1 (1991).

[3] S. Süllow, B. Ludoph, B. Becker, G. J. Nieuwenhuys, A. A. Menovsky, J. A. Mydosh, S. A. M. Mentink, and T. E. Mason, Phys. Rev. B **52**, 12 784 (1995).

[4] R. H. Heffner and M. R. Norman, Comments Condens. Matter Phys. **17**, 361 (1996).

[5] S. Doniach, in *Valence Instabilities and Related Narrow-Band Phenomena*, edited by R. D. Parks (Plenum, New York, 1977), p. 169; Physica B **91**, 231 (1977).

[6] T. Endstra, G. J. Nieuwenhuys, and J. A. Mydosh, Phys. Rev. B **48**, 9585 (1993).
[7] S. A. M. Mentink, G. J. Nieuwenhuys, A. A. Menovsky, J. A. Mydosh, H. Tou, and Y. Kitaoka, Phys. Rev. B **49**, 15 759 (1994).
[8] S. Süllow, B. Ludoph, G. J. Nieuwenhuys, A. A. Menovsky, and J. A. Mydosh, Physica B **223&224**, 208 (1996).
[9] A. Grauel, A. Böhm, H. Fischer, C. Geibel, R. Köhler, R. Modler, C. Schank, F. Steglich, G. Weber, T. Komatsubara, and N. Sato, Phys. Rev. B **46**, 5818 (1992).
[10] S. Teitel and C. Jayaprakash, Phys. Rev. B **27**, 598 (1983).
[11] D. H. Lee, J. D. Joannopoulos, J. W. Negele, and D. P. Landau, Phys. Rev. Lett. **52**, 433 (1984).
[12] C. Geibel, C. Schank, F. Jährling, B. Buschinger, A. Grauel, T. Lühmann, P. Gegenwart, R. Helfrich, P. H. P. Reinders, and F. Steglich, Physica B **199&200**, 128 (1994).
[13] Y. Dalichaouch, M. C. de Andrade, D. A. Gajewski, R. Chau, P. Visani, and M. B. Maple, Phys. Rev. Lett. **75**, 3938 (1995).
[14] R. Balian and R. Werthamer, Phys. Rev. **131**, 1553 (1963).
[15] P. Hirschfeld, D. Vollhardt, and P. Wölfle, Solid State Commun. **59**, 111 (1986).
[16] A. J. Millis, S. Sachdev, and C. M. Varma, Phys. Rev. B **37**, 4975 (1988).
[17] R. Caspary, P. Hellmann, M. Keller, G. Sparn, C. Wassilew, R. Köhler, C. Geibel, C. Schank, F. Steglich, and N. E. Phillips, Phys. Rev. Lett. **71**, 2146 (1993).
[18] H. Tou, Y. Kitaoka, T. Kamatsuka, K. Asayama, C. Geibel, F. Steglich, S. Süllow, and J. A. Mydosh, Physica B **230-232**, 360 (1997).
[19] M. Kyogaku, Y. Kitaoka, K. Asayama, C. Geibel, C. Schank, and F. Steglich, J. Phys. Soc. Jpn. **62**, 4016 (1993).
[20] H. Tou, Y. Kitaoka, K. Asayama, C. Geibel, C. Schank, and F. Steglich, J. Phys. Soc. Jpn. **64**, 725 (1995).